Risk of Colloidal and Pseudo-colloidal Transport of Actinides in Nitrate Contaminated Groundwater nearby radioactive waste repository after bioremediation

ALEXEY SAFONOV (alexeysafonof@gmail.com)
Frumkin Institute of Physical Chemistry and Electrochemistry

Elena Lavrinovich
V.I. Vernadsky Institute of Geochemistry and Analytical Chemistry

Alexander Emel'yanov
V.I. Vernadsky Institute of Geochemistry and Analytical Chemistry

Kirill Boldyrev
Nuclear Safety Institute

Vladimir Kuryakov
Oil and Gas Research Institute

Natalia Rodygina
Frumkin Institute of Physical Chemistry and Electrochemistry

Elena Zakharova
Frumkin Institute of Physical Chemistry and Electrochemistry

Alexander Novikov
V.I. Vernadsky Institute of Geochemistry and Analytical Chemistry

Research Article

Keywords: Actinides, in situ bioremediation, nitrates, colloidal transport, iron and clay particles, filtration, aggregation and coagulation PHREEQC, speciation modeling

Posted Date: March 25th, 2021

DOI: https://doi.org/10.21203/rs.3.rs-348977/v1

Abstract

The possible role of biogeochemical processes in colloidal and pseudo-colloidal U, Np and Pu transport during bioremediation of radionuclide- and nitrate contaminated groundwater was investigated. In two series of laboratory experiments with water samples taken from contaminated aquifer before and past bioremediation we found that microbial processes were able to cause coagulation of clayed, ferruginous and actinide colloids. The main mechanisms are: biogenic insoluble ferrous iron species formation (goethite, pyrrhotite, siderite, troilite, and ferrihydrite sediments), clay particles aggregation by biopolymers, and actinides immobilization in the cells, large biopolimers and iron and clayed sediments. This process results in a decreasing risk of colloidal and pseudo-colloidal transport of actinides.

Highlights

- Microbial stimulation causes formation of new mineral phases and U precipitation
- Microbial processes may cause aggregation and coagulation of suspended particles
- Clayed and ferruginous particles agrégation caused by biopolymers and cells
- in situ bioremediation should prevent risk of actinide colloid transport

Introduction

Improper operations of surface waste storages of radiochemical production plants and ore processing sites, subsurface uranium leaching, radiation accidents, and underground nuclear explosions may all cause the ingress of actinides into groundwater. In Russia, at a number of radiochemical plants, including the Siberian Chemical Combine (SCC) and Mining Chemical Combine, liquid radioactive waste (LRW) is disposed both in deep (250–350 m) collectors [1] and upper open repositories for solid sludges and tales [2, 3, 4]. Since nitrates of alkaline and alkaline-earth elements are the main components of radioactive wastes both in surface depositories and in deep collector layers, radionuclide migration occurs at elevated salt concentrations. The presence of nitrate ions and sulfate ions promotes the oxidative environment in aquifers and a consequent migration of actinides in a dissolved oxidized form [5]. Carbonates contained in the waste create the risks of migration of complex carbonate forms of actinides [6].

The mechanisms of colloidal and pseudo-colloidal transport of actinides under diverse geochemical conditions are of special interest [7, 8]. A number of studies indicate that colloidal transport may play a key role in uranium and plutonium migration both as true colloidal particles and as components of complex particles in ferruginous, clay, or organic complexes [9, 10, 11, 12, 13].

Penetration of nitrates and other components into the surface and submerged water-bearing aquifers may enhance the microbial processes [14, 15]. At some plants, the microbial community was stimulated with organic substrates in order to immobilize uranium and other radionuclides, and to remove nitrates [16; 17; 18]. Multiple studies on bioremediation of uranium-containing waters describe the “biogenic

uraninite" form of uranium IV, commonly as a poorly soluble X-ray amorphous phase. [19, 20]. The formation of several biogenic phosphate phases is also noted [21]. However, no data on similar forms of plutonium and neptunium could be found. The role of biogeochemical processes in colloidal and pseudo-colloidal actinide transport remains insufficiently studied. Biogenic processes stimulated, e.g., by nitrate reduction, may result in stabilization of pseudo-colloidal actinide particles due to production of exopolysaccharide metabolites [22, 23] or biogenic nano colloidal uraninite [24]. The formation of biogenic ferruginous particles [25] may result in the occurrence of new actinide-transporting colloidal phases.

An aquifer nearby the mothballed SCC RW repository which is taken into consideration in the present study was polluted with nitrates and actinides. During 2014–2015, bioremediation of named aquifer was conducted. Bioremediation involved a single stimulation of microbial community with a mixture of acetate and whey. This led to a significant decrease in the redox potential of the system, and to a temporary decrease in nitrate ions concentration to values below the maximum allowable concentrations in in-place conditions [26]. Decreased uranium content was observed in samples taken after the bioremediation, however, precise assessment of uranium forms was impossible. Such results have shown promising perspectives of developing a biogeochemical barrier for radionuclides under conditions of the aquifer in consideration, given continuous stimulation of microbial community and formation of areas with reducing conditions so that elements are immobilized in poorly soluble form. Actinides migration in groundwater after bioremediation requires the development of the multifactor and multi-parametric models, which shall take the consequences of its mineral forms, oxidation states, and species in water, including colloid and pseudocolloides forms. The goal of the present work was to assess the role of metabolic products in water samples taken from aquifer where in-situ bioremediation was conducted previously. The role of named products is to be assessed in experiments that model the bioremediation process under conditions of stability of colloidal and pseudo-colloidal ferruginous and clayey phases containing plutonium, neptunium, and uranium.

Materials And Methods

Two water samples were taken from an aquifer located nearby the suspended surface RAW repository (Siberia, Russia) by means of observation wells (12m depth) after pumping one and a half well volumes. Sample 1 was taken from the area three years after the bioremediation process was conducted. Sample 2 was obtained in the same well before bioremediation. The values of pH, Eh, and salinity were determined at the time of sampling. Table 1 lists the parameters of the samples collected from upper aquifers (10–20 m).

Table 1
Parameters of the groundwater samples, mg/l

Well	**1**	**2**
pH	7,0	6.58
Eh	70	65
Oxidizability, mg O_2/L	0.86	13.10
Salinity	1970.0	3952.0
Fe(total)	1,3	0.25
Na^+	257.0	604.0
K^+	9.8	3.09
Ca^{2+}	109.2	316.60
Mg^{2+}	72,5	63.20
NH_4^+	7.64	< 0,05
NO_3^-	970.0	2517.0
SO_4^{2-}	25,1	172.40
Cl^-	5.37	4.52
HCO_3^-	372.2	231.0
NO_2^-	5.2	< 0.2
α- activity, Bq/L	0.55	12.59
β- activity, Bq/L	8.2	28.7

Molecular hydrogen was used as an electron donor in the first stage of research. After preliminary degassing, hydrogen was introduced into the vials instead of the gas phase. Carbonate ions in the formation fluid served as electron acceptors and as a source of carbon.

At the second stage of laboratory modeling, organic compounds were used as electron donors (1 g/L of sodium acetate and 1 g/l of glucose). Actinides (^{233}U, ^{237}Np, and ^{239}Pu) were used in the concentrations of 10^{-8} M/l. Argon was used as the gas phase in the headspace. A low-mineral solution was used to model the water. Composition of named solution was as follows, mg/L: $NaHCO_3$ – 25.2; $MgSO_4*7H_2O$ – 36.6; $CaCl_2*6H_2O$ – 233.8; and $MgCO_3$ – 3.2. Sample from well 2 was used as the source of natural water

(all model water samples were supplemented with 0.5 mL of natural water as a bacterial microcosm source). Some samples of model water were supplemented with bentonite clay (100 mg/L, 10th Khutor deposit, Khakassia) [27] and 10 mg/L $FeCl_3$. The composition of bentonite clay included 67% of montmorillonite, 6% kaolinite, and 3% illite. The complete list of solutions used in experiments and their designations is as following:

- Model water (MW)
- Model water + organic supplement (MWO)
- Model water + clay (MWCl)
- Model water + clay + organic supplement (MWClO)
- Model water + $FeCl_3$ (MWI)
- Model water + $FeCl_3$ + organic supplement (MWIO)
- Natural water (well 2) (NW)
- Natural water (well 2) + organic supplement (NOW)

Analytical techniques. Concentrations of ^{233}U and ^{239}Pu were determined by alpha-spectrometry, ^{237}Np concentration was determined by the luminescent method [28].

Carbohydrate determination was carried out by the phenol–sulfuric acid method according to Dubois [29]. Optical density was measured at 480 nm.

Cell numbers were determined by light microscopy (×1000).

Eh and pH were determined with an Anion ion meter using the relevant electrodes (Econix Expert).

Organic matter in the liquid was measured using an Elementar Vario EL III elemental analyzer.

The size of the cells, colloidal particles, and zeta potential were determined by the dynamic light scattering method using Photocor Compact-Z particle size and zeta potential analyzer. This method is based on measuring the temporal fluctuations in the scattered light intensity. Light scattering intensity was determined by Zetasizer Nano ZS, Malvern Panalytical.

Organic matter in the liquid was measured using an Elementar Vario EL III elemental analyzer. The size of colloidal particles in the model experiments was determined by step-by-step filtration with syringe-mounted Vladipor filters (2.4, 1.2, 0.8, 0.4, 0.22, 0.1, and 0.05 μm –in diameter).

The speciation of actinides in water samples was assessed by thermodynamic modeling in the PhreeqC 2.1software with *llnl.dat* thermodynamic database [30]. The saturation indices (SI) were determined as follows: $SI = \log IAP - \log K_s$, where IAP is a product of activities of the relevant ions and K_s is the equilibrium constant. At $SI > 0$ formation of the studied phase is predicted. The calculated content of each actinide element per sample was 500 μg.

The microbiological parameters of the collected samples (the number and taxonomic characteristics of microbial communities) were presented in previous articles [26, 31]. The presence of the following bacteria in aquifer samples was revealed: aerobic organotrophic, anaerobic fermenting, iron-reducing, and denitrifying bacteria of the phyla *Proteobacteria* (genera *Acidovorax*, *Simplicispira*, *Thermomonas*, *Thiobacillus*, *Pseudomonas*, *Brevundimonas*, and uncultured *Oxalobacteraceae*), Firmicutes (genera *Bacillus* and *Paenibacillus*), and Actinobacteria (*Candidatus Planktophila*, *Gaiella*).

Results And Discussion

1. Formation of Associative Colloids in water samples, stimulated by H_2

Analysis of total organic content in the groundwater samples before laboratory microbial activation showed its low concentration. For the sample taken from the aquifer area where microbial activation was conducted 3 years prior to the research, concentration did not exceed 15 mg/l. Respective concentration amounted to 5–7 mg/l in samples collected from an area which was not subject to microbial activation previously. Filtration studies (step-by-step filtration, Fig. 1) revealed that more than 50% of organic matter in the sample 1 was represented by suspended particles over 1200 nm in size. These were bacterial cells and other large particles (organic clay and ferrous particles, fulvic and humate acids, etc.).

An organic carbon content of 100 and 200 mg/L was observed in 1 and 2 samples respectively after microbial activation by molecular hydrogen. After day 14 of incubation of the sample 1, microbial processes resulted in decreased content of large organic particles (100–2400 nm) and increased content of the particles below 100 nm in size, which correspond to biogenic and associative colloids. The increase was the sharpest among the fraction of particles smaller than 10 nm (biogenic poly- and oligomers).

The amount of the particles 100–50 and 450–220 nm in size in sample 2 increased after microbial activation; these size ranges correspond to true biocolloidal particles. The contribution of large organic particles (associative colloids and cells) decreased significantly. In this sample, the share colloidal particles (100–50 nm) also increased, while the share of 220–100-nm particles decreased significantly, probably due to their consumption or aggregation into larger fractions. The shares of all large fractions decreased as well. Changes in the intensity of light scattering provided the most relevant information (Table 2).

Table 2
Intensity of light scattering (kHz) by particles of different fractions before and after day 14 of ongoing microbial process in the stratal water

Particle fraction size, nm	1 before	1 after	2 before	2 after
< 2400	28	300	39	100
2400 – 1200	30	47	42	143
1200 – 450	30	50	49	209
450 – 220	48	45	34	187
220 – 100	21	40	33	174
100 – 50	19	20	12	141
> 10	0,5	1,2	0,3	4

In sample 1, 450–220 nm particles (which probably represent clayey aggregates or ferruginous colloidal particles) accounted for the highest intensity. After microbial treatment, the share of other particles increased, and the largest particles (probably cells or agglomerated clayey particles) contributed to light scattering the most. The DLS data on the filtrate from the sample 2 indicates that the particles 1200 – 450 nm in size (likely clayey and iron-clayey aggregates) possibly dominated prior to microbial activation, meanwhile, afterward, intensity of light scattering by colloidal particles of all sizes increased; the 1200–450-nm particles remained predominant and comprised a significant share of medium-sized microbial cells.

2. Modelling of microbial process in the model and real samples with actinides

An increase in the size of particles containing organic matter could be explained by the occurrence of bacterial cells and biogenic particles like and clusters of macromolecules, e.g. proteins, exopolysaccharides, and by physicochemical processes, e.g. adhesion of organic matter to clay and ferruginous particles that cause enlargement and sedimentation of the particles. The second stage of the experiment was conducted in order to examine the mechanisms of the named process more thoroughly.

An increase in the concentration of the biomass, with peak values on day 15 and day 20 for model water and natural water respectively, was observed in samples with additions of organic matter (O) (Table 3).

Table 3
A) Polysaccharide concentrations (mg/L) in the model solutions during incubation. B) biomass (g/l) in the model solutions during incubation, Cell/mL.

Sample	Incubation time, days											
	0		5		10		15		20		30	
	A	B	A	B	A	B	A	B	A	B	A	B
MWO	0,1	0	2	0,2	13	0,24	27	0,19	25	0,12	19	0,04
MWClO	0,11	0	3	0,13	15	0,3	29	0,25	21	0,12	13	0,04
MWIO	0,1	0	3	0,15	17	0,25	33	0,22	29	0,15	16	0,07
NWO	0,13	0	5	0,14	18	0,3	34	0,21	28	0,17	22	0,09

The concentration of polysaccharides in named samples also increased alongside. No significant increase of cells and polysaccharides content was recorded in samples with no organic matter additions.

The average hydrodynamic radii of colloidal particles were obtained on days 3, 7, 14, 21, and 28 of the experiment (Table 4). In model water samples without added organic compounds, colloidal particles were not formed. However, by the end of the experiment particle formation was observed, probably due to the transformation of colloidal matter originating from the natural water aliquot.

Table 4
Hydrodynamic radii of colloidal particles during experiment, nm.

Sample	Incubation time, days				
	5	10	15	20	30
MW	-	-	-	-	20
MWO	90	120	70	40, 170	110
MWCl	130	80	90	100	160
MWClO	130, 25	130	100	100	110
MWI	130	130	100	100	110
MWIO	100	150	160	90	-
NW	75	100	120	120	140
NWO	50	75	90	170	400

In the presence of glucose, the emergence of the colloidal phase and a gradual increase in particle size were observed since the third day of incubation. The average stable hydrodynamic radii of the particles amounted to ~ 100 nm. In the presence of clay, stable colloids with the average hydrodynamic radii of

80–90 nm were formed. Stimulation of microbial processes with glucose resulted in increased particle size and partial sedimentation.

The addition of iron to the model system resulted in the formation of the particles with hydrodynamic radii of ~ 100 nm; the stimulation of the biological processes resulted in increased particle size, the formation of new particles (by day 21), and complete particle sedimentation by day 28.

High diversity in particle size and its gradual, uniform increase were observed in samples without the addition of organic compounds. Under conditions of microbial processes, an increase in particle size was not uniform, and relatively large stable particles (395 nm) were observed at the end of the experiment.

An important parameter used to evaluate the stability of colloidal particles in the system is value of particles' zeta potential. When no organic matter was added, charge of preliminarily filtered 100 – 50 nm particles equaled – 29, -26.2 mV in model water and – 16, -12 mV in natural water, which indicates low stability of such particles (see Table 1 Supplementary). A shift in charge of particles towards zero and positive values was observed when microbial processes were running, and this hints at stabilization of particles in the solution.

The diagrams of actinide distribution by size of colloidal particles in solutions of different nature depending on the incubation time are shown in Fig. 2.

In the model water Pu(IV) forms true colloidal associates (up to 50%) due to deep hydrolytic polymerization. Np(V) was also partially sorbed due to slight disproportionation (by 10%). U(VI) was a stable component of soluble carbonate complexes. In the model water, increased pH and decreased Eh result in the occurrence of 99% Pu, 30% Np, and 10% U within large colloidal particles. Ultrafiltration, however, is not suitable for the assessment of the possible actinide reduction and biosorption contribution to the process of colloid formation.

The microbiota and clay promote stabilization of plutonium and uranium, but not neptunium, in large colloidal particles. The addition of iron had no effect on actinide colloid formation, although iron caused a significant increase in neptunium colloid formation in the presence of the microbiota.

Thus, microbial processes may result in the coagulation of natural colloids due to the development of a weak negative surface charge. The addition of bivalent cations (e.g., Ca^{2+}, Mg^{2+}) during bioremediation should potentiate this process and may become an efficient mechanism for decreasing the risk of active migration of radionuclide-associated particles.

After termination of the biogenic processes, the formation of large uranium-, plutonium-, and neptunium-containing particles associated with cells [32] and large biopolymers (protein-polysaccharide biofilms) [33, 34] polysaccharide-clay and polysaccharide-iron sediments was observed. This results in decreased migration activity of the actinides. Moreover, it is well known that the nucleation process of biogenic iron oxyhydroxides, leading to their mineralization, is closely related to the organic matter of

exopolysaccharides of biofilms Microbial polymers can, through strong mineral binding (high f_{eq}), decrease the nucleation barriers for ferrihydrite and direct nucleation on the polymers [35]. The mineralization process in microbial exopolysaccharide sediments of iron and associated actinides can serve as a reliable anti-migration biogeochemical barrier, an important consequence of bioremediation.

3. Thermodynamical modeling of the Species of Radionuclide Occurrence in the Course of Biotransformation

The data on pH and Eh changes along the process of colloid formation and actinide incorporation into associative particles (and possibly into true colloidal particles as well) are listed in Table 2 (supplementary).

The most notable pH and Eh changes occurred in the presence of the microbiota, which was probably due to increasing in the number of bacteria. The pH increased moderately, while Eh values changed to negative, potentially creating the conditions for a shift of actinides' oxidation states to lower ones. Since Ac(IV) is the most sorbed form of actinides, this may promote their association with colloidal materials of various nature [36].

Speciation of elements, including dissolved species and the phase saturation indices, was calculated for 500 μg/L U, Pu, and Np in the Sample NVO (natural sample 2) (Table 5). The species of actinides and iron after microbial processes were calculated with an account for the following parameter changes: pH increase by 1, Eh decrease by 100 mV, complete denitrification, and sulfate reduction.

Table 5
The major species of actinides and iron in the water from lower aquifer contaminated with radioactive nitrate waste, after microbial treatment

Sample 2, before				
	U	Np	Pu	Fe
Dissolved species, M	$U(OH)_4$ 1.6×10^{-8} UO_2^+ 1.07×10^{-10} **$UO_2(CO_3)_2^{-2}$** 1.13×10^{-6} **$UO_2(CO_3)_3^{-4}$** 7.8×10^{-7} UO_2CO_3 9.4×10^{-8} $UO_2(OH)_2$ 3.8×10^{-8} $(UO_2)_2CO_3(OH)_3^-$ 1.4×10^{-8}	**$Np(OH)_4$** 1.9×10^{-6} $Np(OH)_3^+$ 2.7×10^{-9} **NpO_2^+** 2.0×10^{-7} $NpO_2CO_3^-$ 9.8×10^{-10} NpO_2OH 3.5×10^{-10}	**$PuSO_4^+$** 2.09×10^{-7} $Pu(SO_4)_2^-$ 4.2×10^{-8} $PuOH^{+2}$ 8.1×10^{-9} **$Pu(OH)_4$** 1.3×10^{-7}	**$FeHCO_3^+$** 2.1×10^{-6} $FeSO_4$ 4.1×10^{-8} $FeCO_3$ 3.1×10^{-8} $FeOH^+$ 1.5×10^{-9}
Phase, SI	$UO_{2.25}$(beta) 1.39 $UO_{2.3333}$(beta) 2.36 Uraninite UO_2 1.57	$Np(OH)_4$ 2.63 NpO_2 11.48	$Pu(OH)_4$ 2.19 PuO_2 10.48	Goethite 0.59 Hematite 2.11

	Sample 2, after			
Dissolved species, M	**Solution**			
	Fe	Np	U	Pu
	$FeHCO_3^+$ 1.9×10^{-6}	**$Np(OH)_4$** 2.1×10^{-6}	$U(OH)_4$ 3.0×10^{-8}	$PuOH^{+2}$ 6.0×10^{-10}
	$FeCO_3$ 1.6×10^{-6}	$Np(CO_3)_5^{-6}$ 1.8×10^{-10}	**$UO_2(CO_3)_3^{-4}$** 2.0×10^{-6}	**$Pu(OH)_4$** 2.1×10^{-6}
	$FeOH^+$ 3.6×10^{-8}	NpO_2^+ 2.4×10^{-10}	$UO_2(CO_3)_2^{-2}$ 3.4×10^{-8}	$Pu(OH)_3^+$ 2.2×10^{-10}
	$Fe(OH)_3$ 3.9×10^{-9}	$NpO_2CO_3^-$ 1.4×10^{-10}		
	$Fe(OH)_4^-$ 2.4×10^{-10}			
	Phases			
Phase, SI	Phase	SI	$Np(OH)_4$ 2.67	$UO_{2.25}$ 1.14
	Calcite 1.66	Huntite 1.73	NpO_2 11.53	$UO_{2.25(beta)}$ 1.06
	Aragonite 1.52	Magnesite 0.58	$Pu(OH)_4$ 3.38	$UO_{2.3333(beta)}$ 1.30
	Dolomite 3.97	Monohydrocalcite 0.86	PuO_2 11.67	Uraninite 1.84

Due to thermodynamical modeling experiments after microbial processes, ferrous iron in hydroxide sulphide and carbonate forms were formed, and precipitation of goethite, pyrrhotite, siderite, troilite, and ferrihydrite mineral phases occurred [37, 38, 39, 40]. These new sorption phases could cause additional actinide removal from solutions [41, 42, 43, 44, 45].

Prior to microbial treatment, uranium was expected to be present as di- and tricarbonate complexes. Neptunium occurred as a neptunoyl ion or, as a relatively poorly soluble hydroxo complex. Plutonium was expected to occur as sulfate and as hydroxo complex. Microbial processes resulted in uranium remaining as a tricarbonate complex ore as a poorly soluble hydroxide. Plutonium and neptunium were present in all aquifers as oxyhydroxides, which can be attached to mineral surfaces and various hydroxyl phases [46, 47].

Conclusions

It is important to note that microbial processes resulted in the more extensive formation of poorly soluble phases like uraninite (UO_2, NpO_2, PuO_2). Microbial processes led to occurrence of ferrous iron carbonates and hydrocarbonates, and to the precipitation of goethite, pyrrhotite, siderite, troilite, and ferrihydrite mineral phases. These new sorption phases may result in additional actinide recovery from solutions.

Microbial processes were able to cause coagulation of environmental colloids due to the formation of a weakly negative surface charge. The addition of bivalent cations (e.g., Ca^{2+}, Mg^{2+}) during bioremediation should potentiate this process and may become an efficient mechanism for decreasing the risk of active migration of radionuclide-associated particles [48, 49].

After the termination of biogenic processes, large particles containing uranium, neptunium, and plutonium and associated with the cells and large biopolymers (protein-polysaccharide biofilms) were observed. The occurrence of such particles results in decreased migration activity of the metals. Aggregation of actinide complexes with organic and inorganic colloidal particles in the course of microbial activation results in increased particle size and may hinder their migration in the groundwater-bearing aquifers.

Declarations

This work was supported by State Assignments. 0137-2019-0010 and AAAA-A16-11611091001

The authors have no conflicts of interest to declare that are relevant to the content of this article.

Compliance with Ethical Standards

This research **does not** contain any studies with **human participants** or **animals** performed by any of the authors.

Authors can confirm that all relevant data are included in the article and/or its supplementary information files

Author contributions

A. Safonov, Conceptualization, Investigation, Writing – original draft

E. Lavrinovich, Formal analysis, Investigation

A. Emel'yanov, Formal analysis, Investigation

K. Boldyrev, Formal analysis

V. Kuryakov, Investigation

N. Rodygina, Investigation

E. Zakharova, Conceptualization, Writing – original draft, Supervision

A. Novikov Conceptualization, Writing – original draft, Supervision

References

1. Rybal'chenko, A.I., Pimenov, M.K., Kostin, P.P., et al. (1994). Underground disposal of liquid radioactive wastes (in Russian), Moscow: IZDAT (English Translation by Ben Teague, Sandia National Laboratories, January 1996. Published in 1998 as: Rybalchenko, A.I. (ed). Deep Injection Disposal of Liquid Radioactive Waste in Russia. Richland: Battelle Memorial Institute
2. Safonov A. V., Boguslavsky A. E., Popova N. M. Geochemical Modeling of the Uranium Behavior in Groundwater near the Sludge Storages during Bioremediation. Geochemistry International 59(1):56-65 DOI: 1134/S0016702921010080
3. Krupskaya V. et al. The Influence of Liquid Low-Radioactive Waste Repositories on the Mineral Composition of Surrounding Soils. Sustainability 12(8259) 3390/su12198259 (2020)
4. Boguslavsky A.E., Gaskova O.L., Naymushina O.S., Popova N.M., Safonov A.V. Environmental monitoring of low-level radioactive waste disposal in electrochemical plant facilities in Zelenogorsk, Russia May 2020 Applied Geochemistry 119:104598: 1016/j.apgeochem.2020.104598
5. Wu, W.-M.; et al. Effects of nitrate on the stability of uranium in a bioreduced region of the subsurface. Sci. Technol. 2010, 44, 5104–5111. DOI:10.1021/es1000837
6. Choppin, G.R. Actinide speciation in the environment. J Radioanal Nucl Chem **273,** 695–703 (2007). https://doi.org/10.1007/s10967-007-0933-3
7. Ryan J.N., Elimelech M., Colloid mobilization and transport in groundwater. Colloids and Surfaces, A: Physicochemical and Engineering Aspects, 107 (1996) 1-56 https://doi.org/10.1016/0927-7757(95)03384-X
8. Kersting A.B., et al. Migration of plutonium in ground water at the Nevada Test Site. // Nature. 1999. №397. P.56-59. https://doi.org/10.1038/16231
9. Smith P.A., Degueldre C., Colloid-facilitated transport of radionuclides through fractured media, J. of Contaminant Hydrology 1993, v. 13, p. 143-166. https://doi.org/10.1016/0169-7722(93)90055-W
10. McCarthy J. F., McKay L. D., 2004. Colloid transport in the subsurface. Vadose Zone Journal 310 3(2), 326-337. https://doi.org/10.2113/3.2.326
11. Kurosawa S., Ueta S., Effect of colloids on radionuclide migration for performance assessment of HLW disposal in Japan, Pure Appl. Chem. 2001, v. 73, (12), p. 2027-2037. https://doi.org/10.1351/pac200173122027
12. Flury M., Qiu H., 2008. Modeling colloid-facilitated contaminant transport in the vadose zone. Vadose Zone Journal 7(2), 682-697 DOI: 10.2136/vzj2007.0066
13. Novikov A.P., et al. Colloid Transport of Plutonium in the Far-Field of the Mayak Production Association, Russia. //Science. 2006. V.314. P.638-641. 1126/science.1131307

14. Safonov A. V., Ershov B. G., Gorbunova O. A., Control of microbiological processes during long-term storage of radwastes Atomic Energy, 2012 **112,** 255–260 (2012). https://doi.org/10.1007/s10512-012-9554-1
15. Nazina, T.N. et al. Distribution and activity of microorganisms in the deep repository for liquid radioactive waste at the Siberian Chemical Combine. Microbiology 2006. 75, 727–738 https://doi.org/10.1134/S0026261706060178
16. Vrionis H. A., et al. Microbiological and geochemical heterogeneity in an in situ uranium bioremediation field site. Appl Environ Microbiol 2005;71(10):6308-18. doi: 10.1128/AEM.71.10.6308-6318.2005.
17. Xu, M., et al. Responses of microbial community functional structures to pilot-scale uranium in situ bioremediation. ISME J 4, 1060–1070 (2010). https://doi.org/10.1038/ismej.2010.31
18. Newsome L., Morris K., Lloyd J R. The biogeochemistry and bioremediation of uranium and other priority radionuclides. Chemical Geology https://doi.org/10.1016/j.chemgeo.2013.10.03 Vol 363, Pages 164-184
19. Sharp J.O. et al. Uranium speciation and stability after reductive immobilization in aquifer sediments/ Geochimica et Cosmochimica Acta 75 (2011) 6497–6510 https://doi.org/10.1016/j.gca.2011.08.022
20. Burgos W. D., et al. (2008) Characterization of uraninite nanoparticles produced 6508 J.O. Sharp et al. / Geochimica et Cosmochimica Acta 75 (2011) 6497–6510 by Shewanella oneidensis MR-1. Geochim. Cosmochim. Acta 72(20), 4901–4915
21. Beazley M.J., Martinez R.J., Sobecky P.A., Webb S.M., Taillefert M. Uranium Biomineralization as a Result of Bacterial Phosphatase Activity: Insights from Bacterial Isolates from a Contaminated Subsurface. Environ. Sci. Technol. 2007, 41, 16, 5701–5707 https://doi.org/10.1021/es070567g
22. Tabak, H.H., Lens, P., van Hullebusch, E.D. and Dejonghe, W. Developments in Bioremediation of Soils and Sediments Polluted with Metals and Radionuclides-1. Microbial Processes and Mechanisms Affecting Bioremediation of Metal Contamination and Influencing Metal Toxicity and Transport. Reviews in Environmental Science and Bio/Technology 4:115–156 doi.org/10.1007/s11157-005-2169-4 (2005)
23. Escárcega-González C.E., Garza-Cervantes J.A., Vázquez-Rodríguez A., and Morones-Ramírez J. R.. Bacterial Exopolysaccharides as Reducing and/or Stabilizing Agents during Synthesis of Metal Nanoparticles with Biomedical Applications. International Journal of Polymer Science Volume 2018 https://doi.org/10.1155/2018/7045852
24. Bargar J.R.; Bernier-Latmani R.; Giammar D.E.; Tebo B.M. Biogenic Uraninite Nanoparticles and Their Importance for Uranium Remediation. Elements 4(6) 407-412 1811-5209/08/0004-0407$2.50 DOI: 10.2113/gselements.4.6.407 (2008)
25. Veeramani H. et al. Products of abiotic U(VI) reduction by biogenic magnetite and vivianite. Geochim Cosmochim Acta, Volume 75, Issue 9, 1 May 2011, Pages 2512-2528 https://doi.org/10.1016/j.gca.2011.02.024 (2011)

26. Safonov A.V., et al. Microbial Community and in situ Bioremediation of Groundwater by Nitrate Removal in the Zone of a Radioactive Waste Surface Repository. Frontiers in microbiology 2018, (9)1985, 2-17, 201 https://doi.org/10.3389/fmicb.2018.01985
27. Belousov P.E., Krupskaya V.V. Bentonite clays of Russia and neighboring countries. Georesursy=Georesources, 21(3),pp.79-90. https://doi.org/10.18599/grs.2019.3.79-90 (2019)
28. Novikov A.P., Tkachev V.V., Myasoedov B.F. Speciation methods of actinides in trace concentrations. Comptes Rendus Chimie, 2004 vol 7, № 12, p. 1219-1225 DOI https://doi.org/10.1016/j.crci.2004.05.005
29. Dubois M., Gilles K. A., Hamilton J. K., Rebers P. A., and Smith F. Colorimetric Method for Determination of Sugars and Related Substances. Anal. Chem. 1956, 28, 3, 350–356
30. Parkhurst D. L. et al. User's guide to PHREEQC (Version 2): A computer program for speciation, batch-reaction, one-dimensional transport, and inverse geochemical calculations, 1999
31. Safonov A.V., et al. Biogenic Factors of Radionuclide Immobilization on Sandy Rocks of Upper Aquifers. Radiochemistry 2019, vol 61, № 1, p. 99-108. DOI:10.1134/S0016702919060090
32. J. Panak, et al. X-ray absorption fine structure spectroscopy of plutonium complexes with Bacillus sphaericus. Radiochimica Acta, 90:315–321, 2002.
33. Bin Cao et al. Contribution of extracellular polymeric substances from Shewanella sp. HRCR-1 biofilms to U(VI) immobilization. Environ Sci Technol. 2011 Jul 1;45(13):5483-90. DOI: 10.1021/es200095j
34. Safonov et al. Structure and gene cluster of the O-polysaccharide from Pseudomonas veronii A-6-5 and its uranium bonding. December 2020 International Journal of Biological Macromolecules 165(PtB):2197-2204 DOI:10.1016/j.ijbiomac.2020.10.038
35. Sand K.K. et al. Mechanistic insight into biopolymer induced iron oxide mineralization through quantification of molecular bonding Nanoscale Adv., 2020, 2, 3323-3333 DOI: 10.1039/D0NA00138D
36. Nitsche. Solubility studies of transuranium elements for nuclear waste disposal: Principles and overview. Radiochimica Acta, 52/53:3–8, 1991.
37. Smith D. S. and Ferris F. G.. Specific surface chemical interactions between hydrous ferric oxide and iron-reducing bacteria determined using pKa spectra. Journal of Colloid and Interface Science, 266:60–67, 2003.
38. Kikuchi S et al. Limited reduction of ferrihydrite encrusted by goethite in freshwater sediment. Geobiology. 2016 Jul;14(4):374-89. doi: 10.1111/gbi.12181. Epub 2016 Mar 30. DOI: 10.1111/gbi.12181
39. M. Toner et al. Biogenic iron oxyhydroxide formation at mid-ocean ridge hydrothermal vents: Juan de Fuca Ridge. Geochimica et Cosmochimica Acta Volume73 Issue number 2 388-403 2009
40. V. Chernyshova, S. Ponnurangam, and P. Somasundaran. On the origin of an unusual dependence of (bio)chemical reactivity of ferric hydroxides on nanoparticle size. Physical Chemistry Chemical Physics, 12(42):14045–14056, 2010 2010.

41. Finck N., Nedel S., Dideriksen K., Schlegel M. Trivalent Actinide Uptake by Iron (Hydr)oxides. Environ. Sci. Technol. 2016, 50, 19, 10428–10436 https://doi.org/10.1021/acs.est.6b02599
42. Giammar D. E. and Hering J. G.. Time scales for sorption-desorption and surface precipitation of uranyl on goethite. Environmental Science & Technology, 35(16):3332– 3337, 2001.
43. Gustafsson J. P., Dassman E., and Backstrom M.. Towards a consistent geochemical model for prediction of uranium(VI) removal from groundwater by ferrihydrite. Applied Geochemistry, 24:454–462, 2009.
44. Hixon E., et al. Influence of iron redox transformations on plutonium sorption to sediments. Radiochimica Acta, 98(9-11):685–692, 2010.
45. Moyes L. N., et al. Uranium uptake from aqueous solution by interaction with goethite, lepidocrocite, muscovite, and mackinawite: An X-ray absorption spectroscopy study. Environmental Science & Technology, 34(6):1062–1068, 2000.
46. Kalmykov S. N., Kriventsov V. V., Teterin Y. A., and Novikov A. P. Plutonium and neptunium speciation bound to hydrous ferric oxide colloids. Comptes Rendus Chimie, 10(10-11):1060–1066, 2007.
47. Lu N., Cotter C. R., Kitten H. D, Bentley J., and Triay I. R.. Reversibility of sorption of plutonium-239 onto hematite and goethite colloids. Radiochimica Acta, 83(4):167– 173, 1998
48. Nguyen T.P., Hilala N., Hankins N.P., Novak J. T.. The relationship between cation ions and polysaccharide on the floc formation of synthetic and activated sludge. Desalination Volume 227, Issues 1–3, 30 July 2008, Pages 94-102 https://doi.org/10.1016/j.desal.2007.05.038
49. Joly N, Ghemati D, Aliouche D, Martin P (2020) Interaction of Metal Ions with Mono- and Polysaccharides for Wastewater Treatment: A Review. Nat Prod Chem Res. 8:373. DOI: 10.35248/2329-6836.20.8.373

Figures

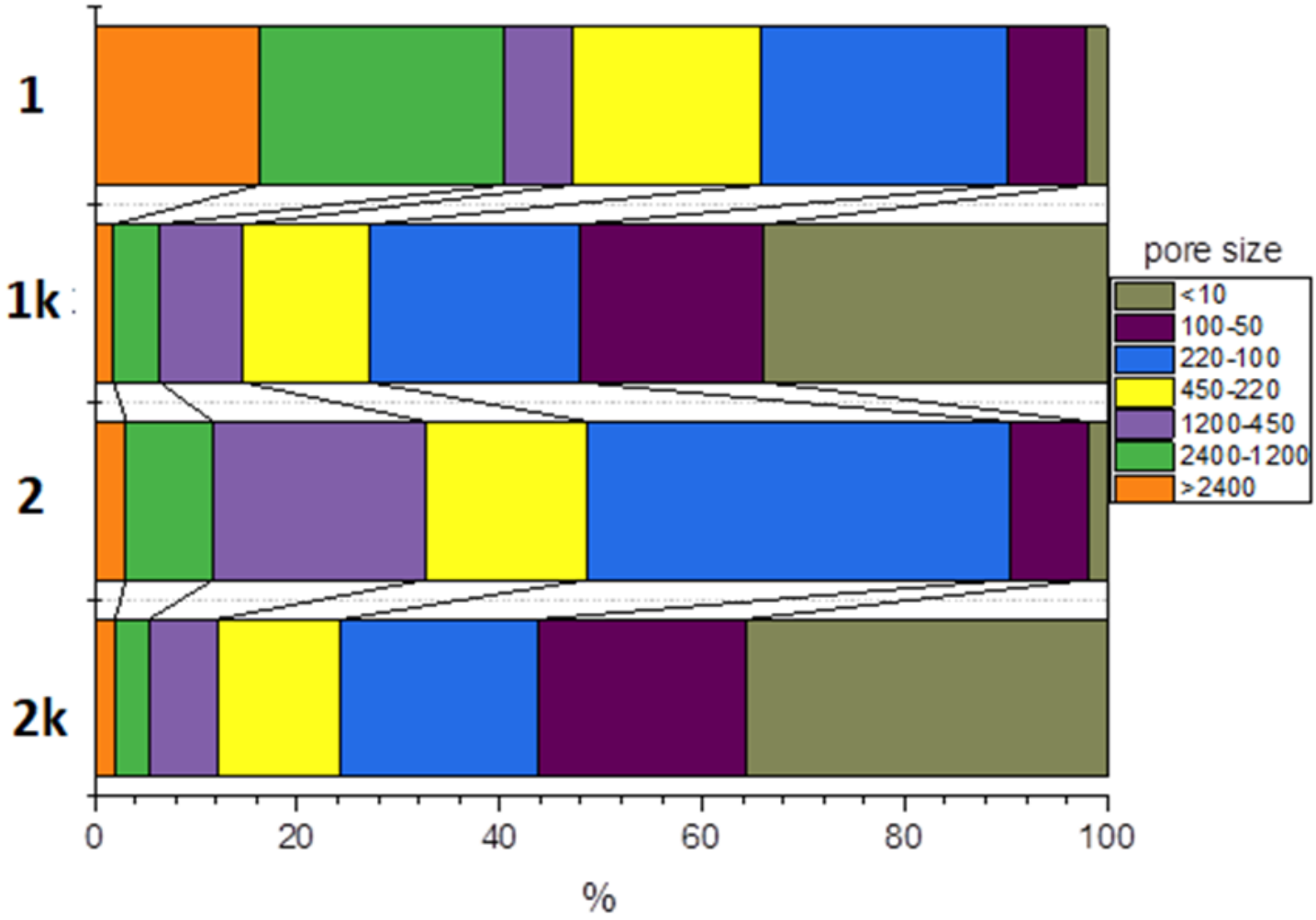

Figure 1

Organic matter distribution by particle size (nm) in samples 1 and 2 before (k) and after microbial activation.

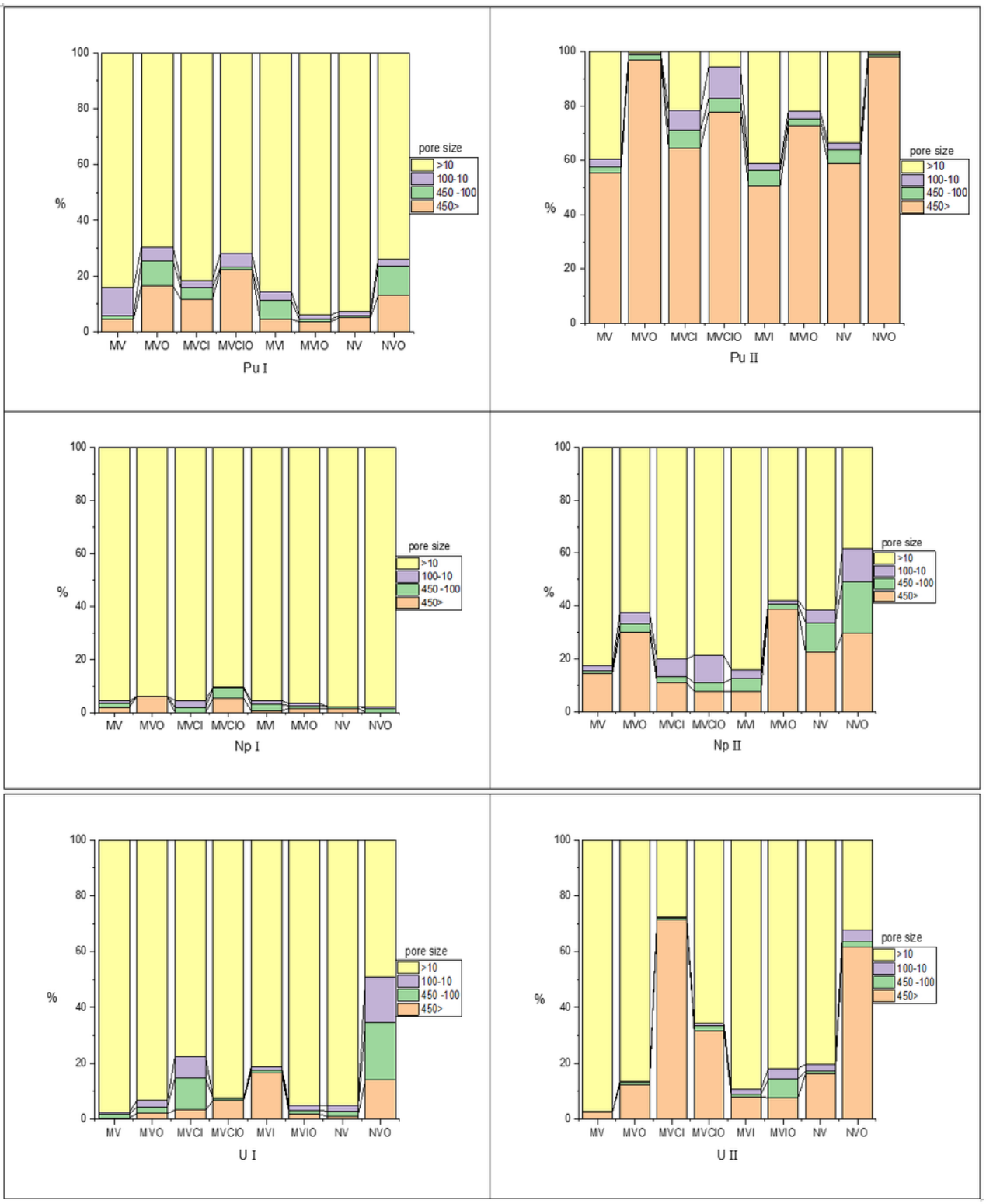

Figure 2

Actinide distribution by size of colloidal particles in solutions of different nature depending on the incubation time, normalized % in the filtrate.

Supplementary Files

This is a list of supplementary files associated with this preprint. Click to download.

- Supplimentary.pdf